

1 **A *Rickettsiella* endosymbiont is a potential source of essential B-**  
2 **vitamins for the poultry red mite, *Dermanyssus gallinae***

6 Daniel R. G. Price<sup>1#</sup>, Kathryn Bartley<sup>1</sup>, Damer P. Blake<sup>2</sup>, Eleanor Karp-Tatham<sup>2</sup>, Francesca  
7 Nunn<sup>1</sup>, Stewart T. G. Burgess<sup>1</sup>, Alasdair J. Nisbet<sup>1</sup>.

10 <sup>1</sup>Moredun Research Institute, Pentlands Science Park, Edinburgh EH26 0PZ, United Kingdom  
11 <sup>2</sup>Pathobiology and Population Sciences, Royal Veterinary College, North Mymms, UK

13 #Correspondence:

16 Moredun Research Institute  
17 Pentlands Science Park  
18 Bush Loan  
19 Penicuik  
20 Midlothian, EH26 0PZ

22 Tel: +44 (0)131 445 5111  
23 Fax: +44 (0)131 445 6111  
24 email: [daniel.price@moredun.ac.uk](mailto:daniel.price@moredun.ac.uk)

38 **Keywords:**

39 Endosymbiont; mutualist; symbiosis; Gammaproteobacteria; vitamin biosynthesis

## 49 **Abstract**

50 Obligate blood-sucking arthropods rely on symbiotic bacteria to provision essential B vitamins  
51 that are either missing or at sub-optimal amounts in their nutritionally challenging blood diet.  
52 The poultry red mite *Dermanyssus gallinae*, an obligate blood-feeding ectoparasite, is  
53 primarily associated with poultry and a serious threat to the hen egg industry. Thus far, the  
54 identity and biological role of nutrient provisioning bacterial mutualists from *D. gallinae* are little  
55 understood. Here, we demonstrate that a *Rickettsiella* Gammaproteobacteria in maternally  
56 transmitted in *D. gallinae* and universally present in *D. gallinae* mites collected at different  
57 sites throughout Europe. In addition, we report the genome sequence of uncultivable  
58 endosymbiont “*Candidatus Rickettsiella rubrum*” from *D. gallinae* eggs. The endosymbiont has  
59 a circular 1.89 Mbp genome that encodes 1973 protein. Phylogenetic analysis confirms the  
60 placement *R. rubrum* within the *Rickettsiella* genus, closely related to a facultative  
61 endosymbiont from the pea aphid and *Coxiella*-like endosymbionts from blood feeding ticks.  
62 Analysis of the *R. rubrum* genome reveals many protein-coding sequences are either  
63 pseudogenized or lost, but *R. rubrum* has retained several B vitamin biosynthesis pathways,  
64 confirming the importance of these pathways in evolution of its nutritional symbiosis with *D.*  
65 *gallinae*. *In silico* metabolic pathway reconstruction revealed that *R. rubrum* is unable to  
66 synthesise protein amino acids and therefore these nutrients are likely provisioned by the host.  
67 In contrast *R. rubrum* retains biosynthetic pathways for B vitamins: thiamine (vitamin B1) via  
68 the salvage pathway; riboflavin (vitamin B2) and pyridoxine (vitamin B6) and the cofactors:  
69 flavin adenine dinucleotide (FAD) and coenzyme A (CoA) that likely provision these nutrients  
70 to the host. We propose that bacterial symbionts which are essential to blood-feeding  
71 arthropod survival provide attractive targets for the development of novel control methods.  
72

## 73 **Introduction**

74 Animals live in a diverse bacterial world and mutualistic associations with bacteria can provide  
75 these animals with novel biochemical traits to exploit an otherwise inaccessible ecological  
76 niche (1). For example, specialist phloem-feeding insects of the order Hemiptera depend on  
77 bacterial endosymbionts to synthesise and provide essential amino acids that are largely  
78 absent in their phloem sap diet (2). Similarly, obligate blood-feeding arthropods, including  
79 insects, ticks and mites associate with nutritional mutualists that provide essential vitamins  
80 and cofactors that are in limited supply from their blood diet [recently reviewed in (3)].  
81 Typically, the microbiome of obligate blood-feeding invertebrates is dominated by a single B  
82 vitamin provisioning symbiont. For example, the obligate blood-feeding African soft tick  
83 (*Ornithodoros moubat*) is associated with a *Francisella* (strain F-Om) mutualist that provides  
84 the host with essential B vitamins to supplement its blood meal diet (4). The genome sequence  
85 of *Francisella* F-Om bears the hallmarks of a typical host-restricted bacterial endosymbiont,  
86 with dramatic genome reduction resulting from loss of redundant genes that are not required  
87 for a symbiotic function. Importantly, *Francisella* F-Om retains biosynthesis pathways for B  
88 vitamins biotin (B7), riboflavin (B2), folic acid (B9) and cofactors coenzyme A (CoA) and flavin  
89 adenine dinucleotide (FAD) to supplement deficiencies in the hosts diet (4). This pattern of  
90 genome reduction and retention of B vitamin biosynthesis pathways is also observed in  
91 *Coxiella*-like endosymbionts (CLEs) from obligate blood-feeding ticks. Recent genome  
92 sequence studies revealed that, in comparison to the non-symbiotic pathogen *C. burnetii*  
93 (genome size 2.03 Mbp), CLEs from ticks have reduced genomes, as small as 0.66 Mbp for  
94 CLE from the lone star tick (CLE of *Amblyomma americanum*), yet they retain pathways for B  
95 vitamin and cofactor biosynthesis to supplement the nutritional requirements of their blood  
96 feeding host (5).

97 The poultry red mite (*Dermanyssus gallinae*) is an obligate blood feeder and a serious

98 threat to the hen egg industry. Throughout Europe, *D. gallinae* prevalence is high, with up to  
99 83% of commercial egg-laying facilities infested (6). Heavy infestations can reach up to  
100 500,000 mites per bird and cause serious welfare issues, including anaemia, irritation and  
101 even death of hens by exsanguination (7). To utilise a blood meal as a single food source, our  
102

103 current hypothesis is that *D. gallinae* associates with nutritional mutualists which synthesize  
104 and supply essential B vitamins and cofactors that are absent in a blood diet. Previous studies  
105 have revealed that *D. gallinae* has a simple microbiome with 10 operational taxonomic units  
106 (OTUs) accounting for between 90% - 99% of the observed microbial diversity (8). Here we  
107 identify a new species of Gammaproteobacteria from the *D. gallinae* microbiome, which we  
108 name “*Candidatus Rickettsiella rubrum*” sp. nov., which is vertically transmitted in *D. gallinae*  
109 and has reached fixation in European *D. gallinae* populations. Genome sequence analysis of  
110 *R. rubrum* reveals a moderately reduced genome of 1.89 Mbp with conserved biosynthesis  
111 pathways for B vitamins including thiamine (vitamin B1), riboflavin (B2), pyridoxine (B6) and  
112 the cofactors flavin adenine dinucleotide (FAD) and coenzyme A (CoA). Thus, *Rickettsiella*  
113 *rubrum* may synthesize and supply *D. gallinae* with essential nutrients that are missing in its  
114 blood diet.

115

116

## 117 **Methods**

### 118 **Mite collection and endosymbiont-enriched DNA preparation**

119 *Dermanyssus gallinae* were collected from a single commercial laying hen facility in the  
120 Scottish Borders, UK and maintained in 75 cm<sup>2</sup> canted tissue culture flasks (Corning Inc.,  
121 Corning, NY, USA) at 4 °C for up to 4 weeks after collection. For experiments requiring mite  
122 eggs, freshly collected mixed stage and gender mites were placed into vented 25 ml Sterilin  
123 universal tubes and maintained at 25 °C, 75% relative humidity in a Sanyo MLR-350H  
124 incubator and eggs were collected the following day.

125 Since obligate bacterial endosymbionts are uncultivable outside the host, bacteria  
126 were derived from *D. gallinae* tissue lysates and host cells depleted using host depletion  
127 solution (Zymo Research, Irvine, CA, USA). Briefly, live mixed life-stage mites were surface  
128 sterilised with 70 % (v/v) ethanol for 30 s at room temperature followed by three 1 min washes  
129 in nuclease-free water. Mites (approx. 25 mg) were then homogenised in 200 µl nuclease-free  
130 water using a tube pestle and host cells lysed by addition of 1 ml of host depletion solution  
131 (Zymo Research, Irvine, CA, USA) with a 15 min incubation at room temperature with end  
132 over end mixing. Intact bacterial cells were pelleted by centrifugation at 10,000 x g for 5 min  
133 at room temp and DNA extracted from the pellet using a DNeasy® Blood & Tissue kit (Qiagen,  
134 Hilden, Germany). DNA concentration was assessed by the Qubit™ dsDNA BR Assay Kit  
135 (Thermo Fisher Scientific, Waltham, MA, USA) and 1% (w/v) agarose gel electrophoresis.

136

### 137 **16S rRNA amplicon sequencing and classification**

138 Poultry red mite eggs were collected as described above and surface sterilised by two 5 min  
139 washes in 0.1% (w/v) benzalkonium chloride followed by two 5 min washes in 70% (v/v)  
140 ethanol. DNA was extracted from eggs using a DNeasy® Blood & Tissue kit (Qiagen, Hilden,  
141 Germany) with a lysozyme pre-treatment to lyse bacterial cells. DNA was quantified using a  
142 NanoDrop™ One spectrophotometer (Thermo Fisher Scientific, Waltham, MA, USA) and DNA  
143 molecular weight determined on a 1% (w/v) agarose/TAE gel. A reagent-only control DNA  
144 extraction was performed in parallel using the same DNA extraction kit.

145 The presence of bacterial DNA in mite eggs was verified by PCR using universal  
146 bacterial 16S rRNA gene primers 27F-short (5'- GAGTTTGATCCTGGCTCA -3') and 1507R  
147 (5'- TACCTTGTACGACTTCACCCAG -3'). Each 50 µl PCR reaction contained template  
148 DNA (100 ng), 1 U Platinum™ Taq DNA Polymerase (Thermo Fisher Scientific, Waltham, MA,  
149 USA), 1x PCR buffer, 1.5 mM MgCl<sub>2</sub>, 0.2 mM of each dNTP and each primer at 0.2 µM. Cycling  
150 conditions were as follows: 94 °C for 2 min; 30 cycles of 94 °C 30 s, 58 °C 30 s, 72 °C 1min  
151 30 s and a final hold of 72 °C for 10 min. A control PCR reaction was performed using the  
152 same conditions with an equivalent volume of eluate from the reagent-only control extraction.  
153 PCR products were cloned into pJET1.2 using the CloneJet PCR cloning kit (Thermo Fisher  
154 Scientific, Waltham, MA, USA) and transformed into chemically competent JM109 *E. coli* cells  
155 (Promega, Madison, WI, USA). Transformants were selected on Lysogeny broth (LB) agar  
156 plates containing 100 µg/ml ampicillin at 37 °C. Colony PCR was performed on randomly

157 selected individual colonies using pJET1.2-F (5'- CGACTCACTATAGGGAGAGCGGC -3')  
158 and pJET1.2-R (5'- AAGAACATCGATTTCCATGGCAG -3') vector primers using the  
159 previously detailed cycling conditions, except the primer annealing temperature was reduced  
160 to 56 °C. PCR products were analysed on a 1% (w/v) agarose/TAE gel and colonies containing  
161 the expected size amplification product were grown overnight in 10 ml LB containing 100 µg/ml  
162 ampicillin at 37 °C with shaking at 200 rpm. Plasmid DNA was isolated from each clone using  
163 Wizard® Plus SV Miniprep kit (Promega, Madison, WI, USA) and a total of 72 individual clones  
164 were sequenced with pJET1.2-F and pJET1.2-R primers at Eurofins Genomics Germany  
165 GmbH.

166 To assess the geographical association between *D. gallinae* and *Rickettsiella* we used  
167 DNA from a previously published mite collection from 63 sites across Europe (9). DNA from  
168 each collection sample was screened for *Rickettsiella* DNA using taxa specific 16S rRNA  
169 primers Rick-F (5'- GTCGAACGGCAGCACGGTAAAGACT -3') and Rick-R (5'-  
170 TCGGTTACCTTCTTCCCCACCTAA -3'), which were designed based on alignments in the  
171 PhyloPD database (10). Each 25 µl PCR reaction contained template DNA (5 ng), 0.5 U  
172 Phusion™ High-Fidelity DNA Polymerase (Thermo Fisher Scientific, Waltham, MA, USA), 1x  
173 PCR buffer, 0.2 mM of each dNTP and each primer at 0.5 µM. Cycling conditions were as  
174 follows: 98 °C for 30 s; 30 cycles of 98 °C 10 s, 68 °C 30 s, 72 °C 30 s and a final hold of 72  
175 °C for 10 min. PCR products were sequenced in both directions using Rick-seq-F (5'-  
176 AACGGCAGCACGGTAAAGAC -3') and Rick-seq-R (5'- AGTGCTTACAACCCGAAGG -3')  
177 sequencing primers at Eurofins Genomics Germany GmbH.

178 16S rRNA sequences were classified with the RDP Classifier 2.13 (training set No. 18)  
179 (11) and sequences with <80% bootstrap support as their genus assignment were removed  
180 from the dataset. All remaining sequences were used in blastn searches against the GenBank  
181 database to identify their top hit.

### 182 **Genome Sequencing and Assembly**

183 Raw PacBio reads generated from DNA isolated from *D. gallinae* eggs (published in (12))  
184 were retrieved; the data set contained 7,318,092 reads for a total of 63,984,748,667 bases.  
185 Raw reads were mapped against the *D. gallinae* reference genome using Minimap2 v.2.17  
186 (13) and unmapped reads were extracted from the resulting BAM files using SAMtools v1.11  
187 (14). Unmapped reads (814,785 reads for a total of 1,274,422,647 bases) were assembled  
188 using the metaFlye assembler v.2.8.2 under default settings using the --pacbio-raw and --meta  
189 flags (15). The assembly containing 652 contigs was visualised with Bandage (16) which  
190 allowed identification of a circular 1.89 Mbp *Rickettsiella* genome with 12x coverage.

191 For massive parallel sequencing (MPS) host-depleted gDNA extracted as described  
192 above, was fragmented using a Covaris system, size-selected for 200 – 400 bp fragments and  
193 used for construction of a single strand DNA circle library. The library was amplified using  
194 phi29 DNA polymerase by rolling circle amplification to make DNA nanoballs (DNBs) and  
195 sequenced on a DNBSEQ-G50 platform as 150 bp paired end reads. Library construction and  
196 sequencing were performed by BGI Genomics (Shenzhen, China). This sequencing effort  
197 resulted in generation of 174,890,018 reads for a total of 26,233,502,700 bases. The reads  
198 were used to polish the *Rickettsiella* consensus sequence. Briefly, short-reads were mapped  
199 to the *Rickettsiella* genome using BWA-MEM aligner v0.7.17 (17) and base calls were  
200 corrected using five iterative rounds of polishing with Pilon v1.23 (18). The resultant assembly  
201 consisted of a single circular chromosome of 1,888,715 bp with 3,712x coverage.

### 202 **Genome Annotation**

203 The genome was annotated using Prokka v.1.14.6 (19) and the automated pipeline included  
204 coding region prediction by Prodigal (20) and annotation of non-coding rRNAs using Barnap  
205 and tRNAs using ARAGORN (21). As part of the Prokka pipeline, insertion sequences (IS)  
206 were annotated using the ISfinder database (22). Metabolic pathways for amino acids, B  
207 vitamins and cofactors were manually constructed using KEGG (23) and MetaCyc (24)  
208 reference pathways as guides and decorated with results from the genome annotation. The

211 absence of genes in pathways was verified by tblastn searches against the *Rickettsiella*  
212 genome. The genome plot was generated using DNAPlotter (25).  
213

#### 214 **Proposal for the species name of *Rickettsiella*-like endosymbiont**

215 We have demonstrated that the symbiont belongs to the genus *Rickettsiella* and has less than  
216 98.7% 16S rRNA sequence identity to its closest named phylogenetic neighbour, suggesting  
217 that the recovered genome is a new species. We propose in accordance with the terms for  
218 species designation for unculturable bacteria the name “*Candidatus Rickettsiella rubrum*” sp.  
219 nov. (hereafter *Rickettsiella rubrum* for simplicity). The specific name “rubrum” refers to the  
220 “red” colour of its mite host, the poultry red mite *Dermanyssus gallinae* after ingestion of a  
221 blood meal.  
222

#### 223 **Phylogenetic analysis**

224 For phylogenetic analysis, full-length 16S rRNA sequences were aligned using ClustalW and  
225 a maximum-likelihood (ML) phylogenetic tree constructed using the Kimura 2-parameter (K2)  
226 model with gamma distributed with invariant sites (G+I). The substitution model was selected  
227 based on BIC score (Bayesian Information Criterion) and reliability of the tree was tested using  
228 bootstrap analysis (1000 replicates) with bootstrap values indicated on the tree. All  
229 phylogenetic analyses were performed using MEGA version X (26).  
230

231

## 232 **Results and Discussion**

### 233 ***Rickettsiella* is maternally inherited in *D. gallinae*.**

234 16S rRNA amplicon sequencing of DNA isolated from surface-sterilised *D. gallinae* eggs  
235 reveals that *Rickettsiella* is detectable in eggs (Figure 1), raising the possibility that  
236 *Rickettsiella* is maternally inherited in *D. gallinae*. It is notable that the *R. rubrum* whole  
237 genome sequence reported here was assembled from PacBio long-reads that were generated  
238 from DNA isolated from surface-sterilised mite eggs. In addition, a recent study of the *D.*  
239 *gallinae* microbiome identified *Rickettsiella* in all life-stages, including eggs, from mites  
240 collected from four geographically isolated commercial laying hen facilities in Czechia (27).  
241 Further attempts were made to assess the *Rickettsiella* transmission rate by running  
242 diagnostic PCR on DNA isolated from individual *D. gallinae* eggs, however, due to the small  
243 egg size and low recovery of DNA it was not possible to assess presence/absence in individual  
244 eggs.  
245

### 246 ***Rickettsiella* infection has reached fixation in European populations of *D. gallinae*.**

247 We performed an extensive diagnostic PCR screen to test *D. gallinae* populations from  
248 collection sites throughout Europe for the presence of *Rickettsiella*. To do this, we used a  
249 previously prepared *D. gallinae* DNA collection extracted from mites sourced from commercial  
250 laying hen facilities from 62 sites across 15 European countries (9). For each sample site, total  
251 *D. gallinae* DNA was isolated from an individual adult mites, according to (9) and each sample  
252 was screened by diagnostic PCR using *Rickettsiella*-specific 16S rRNA primers. DNA samples  
253 from all *D. gallinae* sample sites (n = 62) were *Rickettsiella* positive, indicating that *Rickettsiella*  
254 infection has reached fixation in European *D. gallinae* populations (Figure 2).  
255

### 256 **General features of “*Ca. Rickettsiella rubrum*” genome.**

257 Previously generated PacBio long-read sequence data from *D. gallinae* eggs (12) were used  
258 to assemble the *R. rubrum* genome. From a total of 64.0 Gbp of sequence data, 1.3 Gbp of  
259 reads did not map to the *D. gallinae* draft genome and were used for metagenome assembly,  
260 resulting in generation of 652 contigs, which, after assembly, contained a circular *R. rubrum*  
261 chromosome of 1.89 Mbp. To correct errors associated with long-read sequence data, the *R.*  
262 *rubrum* assembly was polished using five iterative rounds of Pilon with DNBSEQ™ short-read  
263 sequence data from symbiont enriched DNA. This yielded a circular chromosome of 1,888,715  
264 bp with 3,712x coverage and a G+C content of 39.6 % (Figure 3). Based on Prokka gene

265 prediction and annotation, the *R. rubrum* genome has 1,973 protein coding open reading  
266 frames (ORFs) with an average size of 870 bp which covered 91 % of the genome (Table 1  
267 and Supplementary Table 1). Of these ORFs, 970 were assigned a biological function by  
268 Prokka annotation, 585 were annotated by BLAST homology to characterised proteins, while  
269 227 matched hypothetical proteins of unknown function and 191 were unique to *R. rubrum*. In  
270 seven cases, pairs of adjacent genes were annotated with identical names and clearly the  
271 ORF was interrupted by a stop codon splitting the gene into two or more parts (these genes  
272 are highlighted in Supplementary Table 1). It is likely that these fragmented genes are non-  
273 functional and in the early stages of pseudogenization. To identify other pseudogene  
274 candidates we compared the length ratios of each predicted *R. rubrum* protein against their  
275 top blastp hit from searches against the NCBI nr protein database and flagged *R. rubrum*  
276 proteins that deviated by more than +/- 25% (Supplementary Table 1). In summary, out of a  
277 total of 1,973 *R. rubrum* protein coding ORFs searched, only 312 (15.8%) deviate by more  
278 than +/- 25% from their top hit and are candidate pseudogenes. However, it should be noted  
279 that the majority of these pseudogene candidates are “hypothetical proteins” of unknown  
280 function and therefore await experimental validation as genuine loss of function pseudogenes.  
281 We detected 41 tRNA genes (which can translate all 61 amino acid codons), 6 rRNA gene  
282 operons and 19 insertion-sequence (IS) elements.  
283

284 ***R. rubrum* is related to endosymbionts and endoparasites from the order Legionellales.**  
285 All members of the Gammaproteobacteria order Legionellales are host-adapted for  
286 endosymbiotic or endoparasitic lifestyles within eukaryotic cells. Within Legionellales  
287 members of the genus *Rickettsiella* form a monophyletic group that diverged from *Coxiella*  
288 *burnetii*, the etiologic agent of Q fever, approx. 350 million years ago (29). *Rickettsiella* sp. are  
289 found in a wide range of arthropod hosts and are best known as obligate intracellular  
290 pathogens (29, 30), but recently some have been characterised as mutualistic endosymbionts  
291 (31, 32). Phylogenetic analysis, using 16S rRNA gene sequences from representative  
292 Gammaproteobacteria, confirms the placement *R. rubrum* within the *Rickettsiella* genus,  
293 closely related to the facultative endosymbiont *R. viridis* from the pea aphid *Acyrthosiphon*  
294 *pisum* (33) (Figure 4). In aphids, *R. viridis* was isolated from natural aphid populations and  
295 infection is associated with production of blue-green pigment molecules that accumulate in  
296 the host (32). Of particular note, aphids infected with *R. viridis* are not associated with negative  
297 impacts on host fitness and in some aphid strains infection is associated with elevated growth  
298 rates (32). Whole genome alignments between *R. rubrum* and *R. viridis* confirms that these  
299 two bacteria are very closely related but major genomic rearrangements including inversions,  
300 translocations and insertions are apparent (Figure 5).

301 Nutritional endosymbionts of blood-feeding arthropods are abundant in the order  
302 Legionellales. Again, closely related to *R. rubrum*, in the sister-genus *Coxiella* (Figure 4),  
303 *Coxiella*-like endosymbionts (CLEs) are required by ticks for supplementation of B vitamins  
304 that are absent in their blood meal and are essential for tick survival (34). In common with  
305 other host-restricted nutritional endosymbionts of arthropods, CLEs have massively reduced  
306 genomes, retaining functionally non-redundant genes that are essential for the symbiosis.  
307 Recent genome sequencing studies unveiled that, in comparison to *C. burnetii* (genome size  
308 2.03 Mbp), CLEs from ticks exhibit extreme genome reduction, with genomes ranging from  
309 0.66 Mbp for *Coxiella* sp. strain CLEAA (CLE of *Amblyomma americanum*) (5) to 1.73 Mbp for  
310 *Coxiella* sp. strain CRt (CLE of *Rhipicephalus turanicus*) (35). Presumably the range of  
311 genome size among CLEs of blood-feeding ticks reflects an ongoing dynamic process of  
312 reductive genome evolution. Metabolic reconstruction of these reduced genomes reveals  
313 intact B vitamin biosynthesis pathways, required for biosynthesis and provision of these  
314 essential nutrients to the host tick (5, 35).

315 In addition to ticks and mites, the blood-feeding louse *Polyplax serrata* is associated  
316 with a vertically transmitted, host restricted, nutritional endosymbiont from the genus  
317 *Legionella* (36). In comparison to *Legionella pneumophila* (genome size 3.4 Mbp), the etiologic  
318 agent of Legionnaires’ disease, the recently identified endosymbiont *L. polyplacis* has a  
319 massively reduced genome (0.53 Mbp) and parallels the reductive genome evolution

320 observed in CLEs of blood-feeding ticks. Again, in the background of massive genome  
321 reduction *L. polyplacis* retains B vitamin biosynthesis pathways required for biosynthesis and  
322 provision of these essential nutrients to the host insect (36).

323

#### 324 **Genomic reduction in *R. rubrum*: an ongoing process?**

325 Genome reduction is widespread in maternally inherited bacterial endosymbionts and is  
326 associated with loss of genes that are functionally redundant within the host, resulting in  
327 compact endosymbiont genomes containing a subset of genes relative to their free-living  
328 ancestor (37). In general, “ancient” host-restricted endosymbionts have massively reduced  
329 genomes, for example, the smallest known cellular genome of the insect endosymbiont *Nasuia*  
330 *deltoccephalinicola* is a diminutive 112 kbp and encodes just 112 protein coding genes, with  
331 distinctive adaptations to its host (38). In contrast, relatively “recent” host-restricted  
332 endosymbionts have much larger genomes, with gene content more reflective of their closest  
333 free-living ancestor. Following transition to a host-restricted lifestyle the genome of the newly  
334 acquired endosymbiont is associated with a period of genome instability, that typically includes  
335 a large increase in mobile elements in the genome, chromosomal rearrangements mediated  
336 by recombination between mobile elements and an increased pseudogene frequency (39, 40).

337 The genome of *R. rubrum* (1.89 Mbp) is only moderately reduced in comparison to  
338 closely related *C. burnetii* (2.03 Mbp) (Table 1), although it should be noted that *C. burnetii* is  
339 already host-adapted as an obligate intracellular parasite and as such, compared to free-living  
340 bacteria it has a degenerate genome (41). Relative to *C. burnetii*, the CLEs from blood-feeding  
341 ticks have further reduced genomes, typical of reduced genomes observed in other obligate  
342 nutritional endosymbionts of other blood-feeding insects and ticks, where the retained genes  
343 contribute to synthesis of essential B vitamins that are limited in the blood diet of their host  
344 (36, 42, 43, 4, 44). Perhaps the most striking example of genome reduction, in the transition  
345 from a pathogen to a nutritional mutualist, is the loss of virulence associated secretion  
346 systems: In the pathogens *C. burnetii* and *L. pneumophila* the type IV Dot/Icm secretion system  
347 (T4SS) functions to export a suite of virulence factors that modulate host physiology and are  
348 essential for establishment and maintenance of infection (41, 45, 46). Intriguingly, the  
349 massively reduced genomes of CLEAA and Ca. *Legionella* *polyplacis* from the blood feeding  
350 louse *Polyplax serrata* do not encode a Dot/Icm type IVB secretion system and presumably  
351 this secretion apparatus is not required in these nutritional mutualists (36, 5). In contrast,  
352 components of the Dot/Icm type IVB secretion system are retained in *R. rubrum* and are  
353 present in the closely related genomes of *R. viridis* and *R. gyrrilli*, although the sequences of  
354 core components are highly divergent when compared with *C. burnetii* orthologs (Figure 6). It  
355 therefore remains to be determined if the Dot/Icm type IVB secretion system is functional in  
356 *R. rubrum* and if so what role it plays in cellular interactions with the host.

357 Genomes of other obligate intracellular bacteria typically have very few or no insertion  
358 (IS) elements, presumably due to the lack of opportunity for horizontal gene transfer (47, 48).  
359 In contrast, *R. rubrum* contains 19 IS elements evenly distributed around the genome and  
360 there are 8 copies of IS256 family transposase; 4 IS481; 4 ISNCY and 3 IS5. In addition, there  
361 is evidence of extensive horizontal gene transfer (HGT) within *R. rubrum* genome, including  
362 transfers from arthropods (2 HGT events), metazoa (6 HGT events), and numerous transfers  
363 from bacteria outside of Legionellales. Thus, the *R. rubrum* genome is highly dynamic as  
364 evident from the high number of HGT events, numerous IS elements and structural  
365 rearrangements in the *R. rubrum* genome relative to *R. viridis* (Figure 5). Based on these  
366 observations we conclude that *R. rubrum* is recently host-restricted with a genome of similar  
367 size to *C. burnetii* and is yet to undergo significant genome reduction as seen in other related  
368 blood-feeding CLE endosymbionts (5, 35).

369

#### 370 **Metabolic capacity of *R. rubrum*: a putative nutritional mutualist**

371 The *R. rubrum* genome, as with the related endocellular facultative symbiont *R. viridis*,  
372 retains genes for basic cellular processes including translation, replication, cell wall  
373 biosynthesis and energy production (Figure 7). In Supplementary Table S2, we provide a more  
374 detailed comparative gene content analysis between *R. rubrum* and genomes of *R. viridis* and

375 *C. burnetii* using the pathway/gene list published by (38, 49). Surprisingly, both *R. rubrum* and  
376 *R. viridis* have a fragmented phospholipid biosynthesis pathway, suggesting that they are  
377 unable to complete *de novo* phospholipid biosynthesis. As phospholipid is an indispensable  
378 component of the cell membrane, phospholipid must either be imported from the host or the  
379 fragmented pathway is completed using host imported enzymes.

380 Metabolic reconstruction of amino acid biosynthesis pathways revealed that *R. rubrum*  
381 is unable to synthesize protein amino acids and therefore these nutrients are likely provisioned  
382 by the host (Figure 8). The biosynthesis pathway for the essential amino acid arginine is  
383 mostly complete (8/9 required genes present), although precursor aspartic acid is not  
384 synthesized by *R. rubrum* and the bifunctional aspartokinase/homoserine dehydrogenase 1  
385 (encoded by *thrA*) is missing, again suggesting this pathway is non-functional. Given that *D.*  
386 *gallinae* feeds on blood and is able to digest haemoglobin to release free amino acids (50), it  
387 likely has an excess of essential and non-essential amino acids that meet its own nitrogen  
388 requirements and those of *R. rubrum*. Indeed, in other nutritional endosymbionts of obligate  
389 blood feeding arthropods, amino acid biosynthesis pathways are absent and it is likely the  
390 host supplies amino acids to the endosymbiont (5, 4, 45).

391 Obligate blood feeding arthropods such as the human body louse (*Pediculus*  
392 *humanus*) (42), African soft tick (*Ornithodoros moubata*) (4) and the Lone star tick  
393 (*Amblyomma americanum*) (5) depend on nutritional endosymbionts to synthesize and  
394 provide B vitamins that are available in trace amounts in mammalian blood [reviewed in (3)].  
395 To determine whether *R. rubrum* can play a similar role in *D. gallinae* we surveyed the *R.*  
396 *rubrum* genome for B vitamin biosynthesis genes. The *R. rubrum* genome has conserved  
397 genes involved in the biosynthesis of seven B vitamins, including complete biosynthetic  
398 pathways for thiamine (vitamin B1) via the salvage pathway, riboflavin (vitamin B2), pyridoxine  
399 (vitamin B6) and the cofactors flavin adenine dinucleotide (FAD) and coenzyme A (CoA)  
400 (Figure 8). The biosynthesis pathway for biotin (vitamin B7) is largely complete (9/10 genes  
401 present) although it is missing *bioH*, which is required for pimeloyl-CoA synthesis. The  
402 annotated biotin biosynthesis pathway is based on that of the model organism *E. coli*, where  
403 *bioC* and *bioH* are required for synthesis of the intermediate pimeloyl-CoA. However, unlike  
404 the representative “*bioC/bioH*” pathway of *E. coli* many *bioC*-containing microorganisms lack  
405 *bioH* homologues, raising the possibility of non-homologous gene replacement in some  
406 bacteria (51). To date, there are five documented cases of *bioH* gene replacement, which  
407 includes *bioK* of *Synechococcus* (51), *bioG* of *Haemophilus influenzae* (51), *bioJ* of *Francisella*  
408 *sp.* (52), *bioV* of *Helicobacter* *sp.* (53) and *bioZ* of *Agrobacterium tumefaciens* (54). Further  
409 *tblastn* searches against the *R. rubrum* genome using *bioH* and the non-homologous gene  
410 replacements *bioK*, *bioG*, *bioJ*, *bioV* did not identify gene products that can fill the *bioH* gap.  
411 However, a gene encoding ketoacyl-ACP synthase (KAS) III from *R. rubrum* has similarity to  
412 *bioZ* of *A. tumefaciens* and is therefore a candidate to replace *bioH*. Given the retention of a  
413 long biotin biosynthesis pathway in *R. rubrum* (9/10 genes present) and the propensity for the  
414 missing *bioH* gene to be replaced in other bacteria, we predict that the biotin biosynthesis  
415 pathway is functional in *R. rubrum*. In contrast, the other B vitamin biosynthesis pathways for  
416 nicotinic acid (vitamin B3), pantothenic acid (vitamin B5) and folic acid (vitamin B9) are more  
417 fragmented and thus may be non-functional. Although *R. rubrum* biosynthesis pathways for  
418 vitamin B3, B5 and B9 are fragmented future work will analyse these pathways in the context  
419 of the *R. rubrum* metagenome. Genome analyses of other nutritional endosymbionts reveal  
420 that some retained “broken” pathways are functional with gene products supplemented from  
421 multiple species of symbiont partners resulting in metabolic mosaics for the synthesis of  
422 essential nutrients (55, 56). We know from 16S rRNA amplicon sequencing that the *D. gallinae*  
423 microbiome is relatively simple, with 10 OTUs accounting for between 90% - 99% of the  
424 microbial diversity observed (8). Currently, the contribution of other partners in the *D. gallinae*  
425 microbiome towards B vitamin biosynthesis is unknown and will be the target of future studies.

426  
427  
428  
429

430 **References**

- 431 1. M. McFall-Ngai, *et al.*, Animals in a bacterial world, a new imperative for the life  
432 sciences. *PNAS* **110**, 3229–3236 (2013).
- 433 2. N. A. Moran, Symbiosis as an adaptive process and source of phenotypic complexity.  
434 *PNAS* **104**, 8627–8633 (2007).
- 435 3. F. Husnik, Host-symbiont-pathogen interactions in blood-feeding parasites: nutrition,  
436 immune cross-talk and gene exchange. *Parasitology* **145**, 1294–1303 (2018).
- 437 4. O. Duron, *et al.*, Tick-Bacteria Mutualism Depends on B Vitamin Synthesis Pathways.  
438 *Current Biology* **28**, 1896–1902.e5 (2018).
- 439 5. T. A. Smith, T. Driscoll, J. J. Gillespie, R. Raghavan, A *Coxiella*-like endosymbiont is a  
440 potential vitamin source for the Lone Star tick. *Genome Biol Evol* **7**, 831–838 (2015).
- 441 6. D. R. George, *et al.*, Should the poultry red mite *Dermanyssus gallinae* be of wider  
442 concern for veterinary and medical science? *Parasites & Vectors* **8**, 178 (2015).
- 443 7. A. Sigognault Flochlay, E. Thomas, O. Sparagano, Poultry red mite (*Dermanyssus*  
444 *gallinae*) infestation: a broad impact parasitological disease that still remains a  
445 significant challenge for the egg-laying industry in Europe. *Parasit Vectors* **10** (2017).
- 446 8. J. Hubert, *et al.*, Comparison of Microbiomes between Red Poultry Mite Populations  
447 (*Dermanyssus gallinae*): Predominance of Bartonella-like Bacteria. *Microb Ecol* **74**,  
448 947–960 (2017).
- 449 9. E. Karp-Tatham, *et al.*, Phylogenetic Inference Using Cytochrome C Oxidase Subunit I  
450 (COI) in the Poultry Red Mite, *Dermanyssus gallinae* in the United Kingdom Relative  
451 to a European Framework. *Front. Vet. Sci.* **7** (2020).
- 452 10. F. Jaziri, *et al.*, PhylOPDb: a 16S rRNA oligonucleotide probe database for prokaryotic  
453 identification. *Database (Oxford)* **2014**, bau036 (2014).
- 454 11. Q. Wang, G. M. Garrity, J. M. Tiedje, J. R. Cole, Naive Bayesian classifier for rapid  
455 assignment of rRNA sequences into the new bacterial taxonomy. *Appl Environ  
456 Microbiol* **73**, 5261–5267 (2007).
- 457 12. S. T. G. Burgess, *et al.*, Draft Genome Assembly of the Poultry Red Mite,  
458 *Dermanyssus gallinae*. *Microbiol Resour Announc* **7** (2018).
- 459 13. H. Li, Minimap2: pairwise alignment for nucleotide sequences. *Bioinformatics* **34**,  
460 3094–3100 (2018).
- 461 14. H. Li, *et al.*, The Sequence Alignment/Map format and SAMtools. *Bioinformatics* **25**,  
462 2078–2079 (2009).
- 463 15. M. Kolmogorov, *et al.*, metaFlye: scalable long-read metagenome assembly using  
464 repeat graphs. *Nature Methods* **17**, 1103–1110 (2020).
- 465 16. R. R. Wick, M. B. Schultz, J. Zobel, K. E. Holt, Bandage: interactive visualization of de  
466 novo genome assemblies. *Bioinformatics* **31**, 3350–3352 (2015).
- 467 17. H. Li, Aligning sequence reads, clone sequences and assembly contigs with BWA-  
468 MEM. *arXiv:1303.3997 [q-bio]* (2013) (February 12, 2021).
- 469 18. B. J. Walker, *et al.*, Pilon: An Integrated Tool for Comprehensive Microbial Variant  
470 Detection and Genome Assembly Improvement. *PLOS ONE* **9**, e112963 (2014).
- 471 19. T. Seemann, Prokka: rapid prokaryotic genome annotation. *Bioinformatics* **30**, 2068–  
472 2069 (2014).
- 473 20. D. Hyatt, *et al.*, Prodigal: prokaryotic gene recognition and translation initiation site  
474 identification. *BMC Bioinformatics* **11**, 119 (2010).
- 475 21. D. Laslett, B. Canback, ARAGORN, a program to detect tRNA genes and tmRNA  
476 genes in nucleotide sequences. *Nucleic Acids Res* **32**, 11–16 (2004).
- 477 22. P. Siguier, J. Perochon, L. Lestrade, J. Mahillon, M. Chandler, ISfinder: the reference  
478 centre for bacterial insertion sequences. *Nucleic Acids Res* **34**, D32–36 (2006).
- 479 23. M. Kanehisa, S. Goto, KEGG: Kyoto Encyclopedia of Genes and Genomes. *Nucleic  
480 Acids Res* **28**, 27–30 (2000).
- 481 24. R. Caspi, *et al.*, MetaCyc: a multiorganism database of metabolic pathways and  
482 enzymes. *Nucleic Acids Res* **34**, D511–D516 (2006).

483 25. T. Carver, N. Thomson, A. Bleasby, M. Berriman, J. Parkhill, DNAPlotter: circular and  
484 linear interactive genome visualization. *Bioinformatics* **25**, 119–120 (2009).

485 26. S. Kumar, G. Stecher, M. Li, C. Knyaz, K. Tamura, MEGA X: Molecular Evolutionary  
486 Genetics Analysis across Computing Platforms. *Molecular Biology and Evolution* **35**,  
487 1547–1549 (2018).

488 27. J. Hubert, *et al.*, Comparison of Microbiomes between Red Poultry Mite Populations  
489 (*Dermanyssus gallinae*): Predominance of *Bartonella*-like Bacteria. *Microb Ecol* **74**,  
490 947–960 (2017).

491 28. E. Katsavou, *et al.*, Identification and geographical distribution of pyrethroid resistance  
492 mutations in the poultry red mite *Dermanyssus gallinae*. *Pest Management Science*  
493 **76**, 125–133 (2020).

494 29. R. Cordaux, *et al.*, Molecular Characterization and Evolution of Arthropod-Pathogenic  
495 *Rickettsiella* Bacteria. *Appl. Environ. Microbiol.* **73**, 5045–5047 (2007).

496 30. A. Leclerque, R. G. Kleespies, Type IV secretion system components as phylogenetic  
497 markers of entomopathogenic bacteria of the genus *Rickettsiella*. *FEMS Microbiology  
498 Letters* **279**, 167–173 (2008).

499 31. O. Duron, *et al.*, The Recent Evolution of a Maternally-Inherited Endosymbiont of  
500 Ticks Led to the Emergence of the Q Fever Pathogen, *Coxiella burnetii*. *PLOS  
501 Pathogens* **11**, e1004892 (2015).

502 32. T. Tsuchida, *et al.*, Symbiotic Bacterium Modifies Aphid Body Color. *Science* **330**,  
503 1102–1104 (2010).

504 33. N. Nikoh, *et al.*, Genomic Insight into Symbiosis-Induced Insect Color Change by a  
505 Facultative Bacterial Endosymbiont, “*Candidatus Rickettsiella viridis*.” *mBio* **9** (2018).

506 34. M. G. Guizzo, *et al.*, A *Coxiella* mutualist symbiont is essential to the development of  
507 *Rhipicephalus microplus*. *Scientific Reports* **7**, 17554 (2017).

508 35. Y. Gottlieb, I. Lalzar, L. Klasson, Distinctive Genome Reduction Rates Revealed by  
509 Genomic Analyses of Two *Coxiella*-Like Endosymbionts in Ticks. *Genome Biol Evol* **7**,  
510 1779–1796 (2015).

511 36. J. Říhová, E. Nováková, F. Husník, V. Hypša, Legionella Becoming a Mutualist:  
512 Adaptive Processes Shaping the Genome of Symbiont in the Louse *Polyplax serrata*.  
513 *Genome Biology and Evolution* **9**, 2946–2957 (2017).

514 37. J. P. McCutcheon, N. A. Moran, Extreme genome reduction in symbiotic bacteria.  
515 *Nature Reviews Microbiology* **10**, 13–26 (2012).

516 38. G. M. Bennett, N. A. Moran, Small, Smaller, Smallest: The Origins and Evolution of  
517 Ancient Dual Symbioses in a Phloem-Feeding Insect. *Genome Biol Evol* **5**, 1675–  
518 1688 (2013).

519 39. A. I. Garber, *et al.*, The evolution of interdependence in a four-way mealybug  
520 symbiosis. *bioRxiv*, 2021.01.28.428658 (2021).

521 40. N. A. Moran, G. R. Plague, Genomic changes following host restriction in bacteria.  
522 *Curr Opin Genet Dev* **14**, 627–633 (2004).

523 41. R. Seshadri, *et al.*, Complete genome sequence of the Q-fever pathogen *Coxiella  
524 burnetii*. *PNAS* **100**, 5455–5460 (2003).

525 42. E. F. Kirkness, *et al.*, Genome sequences of the human body louse and its primary  
526 endosymbiont provide insights into the permanent parasitic lifestyle. *PNAS* **107**,  
527 12168–12173 (2010).

528 43. N. Nikoh, *et al.*, Evolutionary origin of insect-Wolbachia nutritional mutualism. *Proc  
529 Natl Acad Sci U S A* **111**, 10257–10262 (2014).

530 44. R. V. M. Rio, *et al.*, Insight into the transmission biology and species-specific  
531 functional capabilities of tsetse (Diptera: glossinidae) obligate symbiont  
532 *Wigglesworthia*. *mBio* **3** (2012).

533 45. M. Chien, *et al.*, The Genomic Sequence of the Accidental Pathogen *Legionella  
534 pneumophila*. *Science* **305**, 1966–1968 (2004).

535 46. L. Gomez-Valero, *et al.*, More than 18,000 effectors in the *Legionella* genus genome  
536 provide multiple, independent combinations for replication in human cells. *PNAS* **116**,  
537 2265–2273 (2019).

538 47. I. L. G. Newton, S. R. Bordenstein, Correlations Between Bacterial Ecology and  
539 Mobile DNA. *Curr Microbiol* **62**, 198–208 (2011).

540 48. I. Tamas, *et al.*, 50 Million Years of Genomic Stasis in Endosymbiotic Bacteria.  
541 *Science* **296**, 2376–2379 (2002).

542 49. N. A. Moran, J. P. McCutcheon, A. Nakabachi, Genomics and Evolution of Heritable  
543 Bacterial Symbionts. *Annual Review of Genetics* **42**, 165–190 (2008).

544 50. D. R. G. Price, *et al.*, Evaluation of vaccine delivery systems for inducing long-lived  
545 antibody responses to *Dermanyssus gallinae* antigen in laying hens. *Avian Pathol* **48**,  
546 S60–S74 (2019).

547 51. M. M. Shapiro, V. Chakravarty, J. E. Cronan, Remarkable Diversity in the Enzymes  
548 Catalyzing the Last Step in Synthesis of the Pimelate Moiety of Biotin. *PLOS ONE* **7**,  
549 e49440 (2012).

550 52. Y. Feng, *et al.*, A *Francisella* virulence factor catalyses an essential reaction of biotin  
551 synthesis. *Mol Microbiol* **91**, 300–314 (2014).

552 53. H. Bi, L. Zhu, J. Jia, J. E. Cronan, A Biotin Biosynthesis Gene Restricted to  
553 *Helicobacter*. *Scientific Reports* **6**, 21162 (2016).

554 54. Y. Hu, J. E. Cronan,  $\alpha$ -proteobacteria synthesize biotin precursor pimeloyl-ACP using  
555 *BioZ* 3-ketoacyl-ACP synthase and lysine catabolism. *Nature Communications* **11**,  
556 5598 (2020).

557 55. J. P. McCutcheon, B. R. McDonald, N. A. Moran, Convergent evolution of metabolic  
558 roles in bacterial co-symbionts of insects. *PNAS* **106**, 15394–15399 (2009).

559 56. F. Husnik, *et al.*, Horizontal gene transfer from diverse bacteria to an insect genome  
560 enables a tripartite nested mealybug symbiosis. *Cell* **153**, 1567–1578 (2013).

561

## 562 **Conflict of Interest**

563 The authors declare that the research was conducted in the absence of any commercial or  
564 financial relationships that could be construed as a potential conflict of interest.

565

## 566 **Author Contributions**

567 DRGP, AJN, STGB conceived the study. All authors designed the research. DRGP, EKT  
568 performed research. DRGP, AJN, STGB analysed data. DRGP wrote the paper with  
569 contributions from all authors. All authors read and approved the final manuscript.

570

## 571 **Data availability statement**

572 DNBseq reads were deposited to the Sequence Read Archive (SRA), under NCBI BioProject  
573 PRJNAXXXXX. The *R. rubrum* genome assembly is available under NCBI BioProject  
574 PRJNAXXXXX.

575

## 576 **Funding**

577 The work was supported in part by a Moredun Foundation Research fellowship awarded to  
578 DRGP and a British Egg Marketing Board (BEMB) Trust PhD scholarship awarded to EKT.

579

## 580 **Acknowledgements**

581 We thank the Bioservices Group at Moredun Research Institute for their ongoing help and  
582 expertise and UK farmers for allowing access to sites for *D. gallinae* collection.

583

584

585

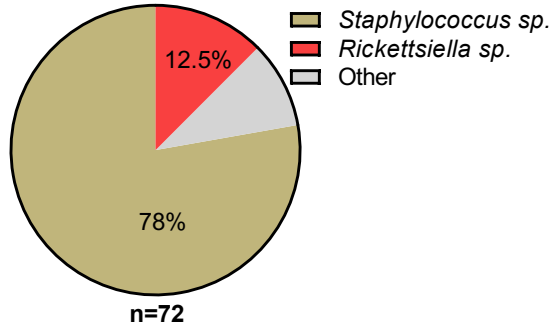
586

587

588

589 **Figures and Figure Legends**

590  
591  
592  
593



594  
595

596 **Figure 1.** Classification and relative abundance of bacteria associated with *D. gallinae* eggs.  
597 The presence of bacterial DNA in mite eggs was verified by PCR using universal bacterial 16S  
598 rRNA gene primers. Amplicons were sequenced (n = 72) and classified with the RDP Classifier  
599 2.13 (training set No. 18). Sequences with <80% bootstrap support as their genus assignment  
600 were removed from the dataset. Classifications are as indicated in the legend, other (grey)  
601 represents single hits (n = 1) to the following genera: *Blautia*; *Clostridium XII*; *Devosia*;  
602 *Paenacaligenes*; *Salinicoccus*; *Streptococcus* and *Tsukamurella*.

603  
604  
605  
606  
607  
608

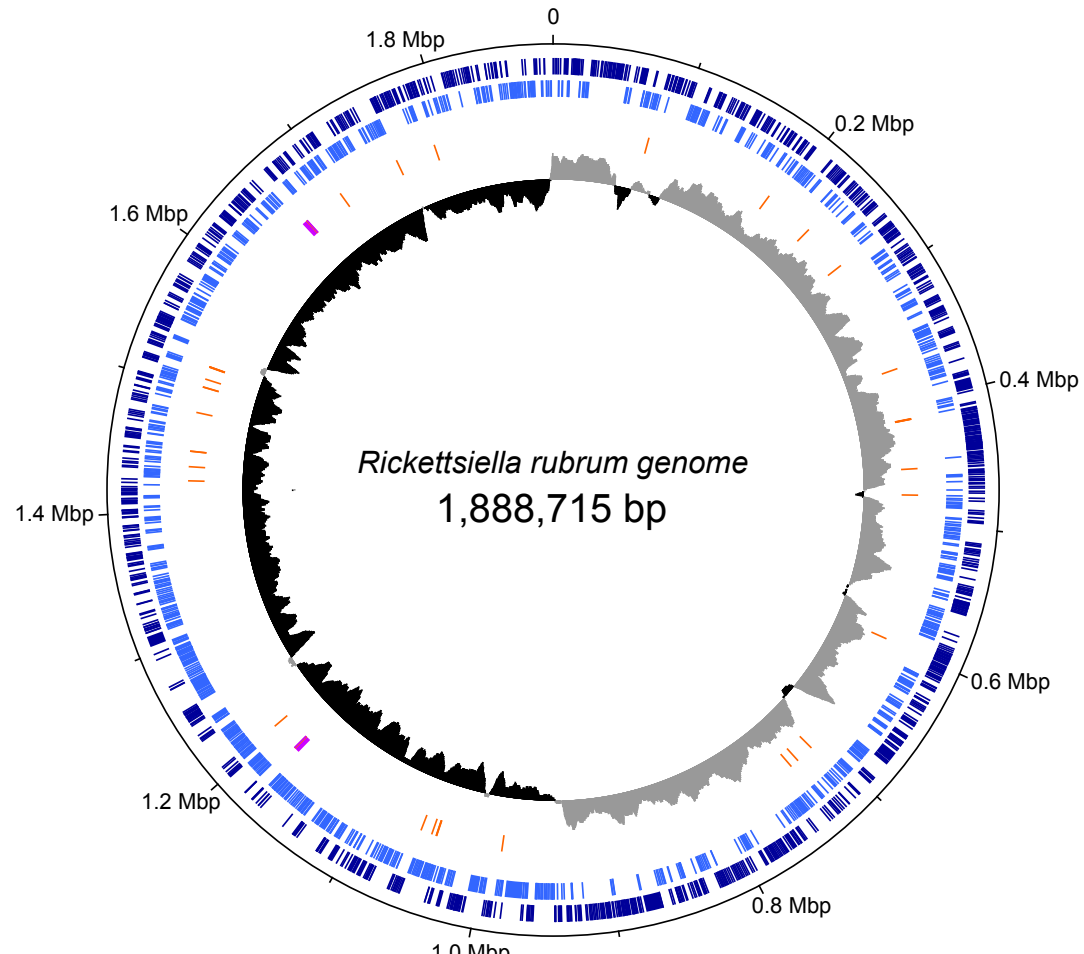


609  
610

611 **Figure 2.** Map showing the distribution of *D. gallinae* populations analysed in this study. All  
612 individual adult female *D. gallinae* mites from each sampling site (63 sites across Europe)  
613 were positive for *Rickettsiella* infection (red circle) indicating *Rickettsiella* infection has  
614 reached fixation in European *D. gallinae* populations.

615  
616

617



618

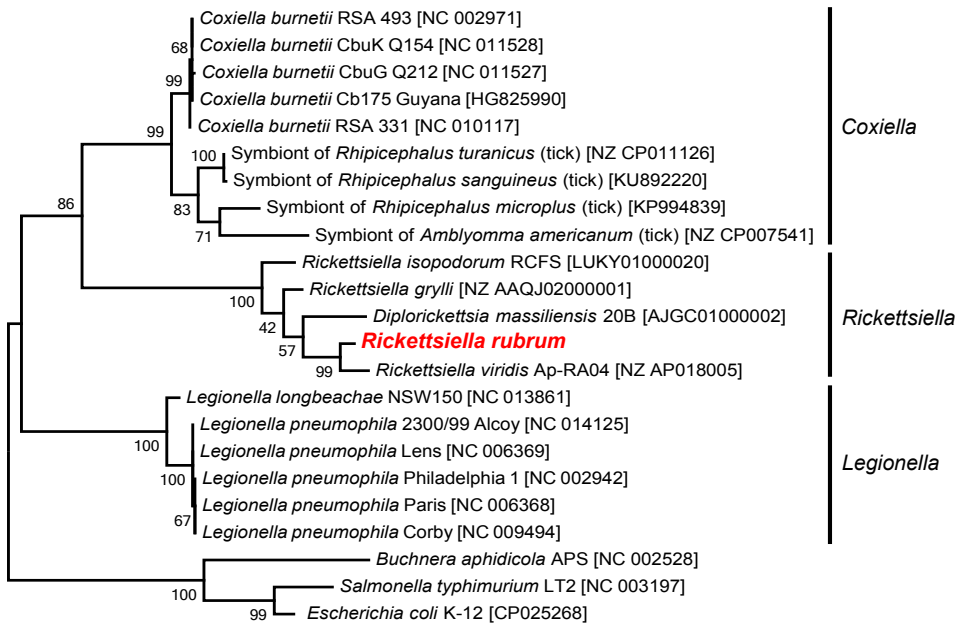
619

620 **Figure 3.** Map of the circular chromosome of "ca. *Rickettsiella rubrum*". The innermost circle  
621 shows GC skew (window size: 10,000 bp) with grey and black indicating high ( $>0$ ) and low  
622 ( $<0$ )  $(G-C)/(G+C)$  values. The second circle shows the positions of tRNA genes (orange) and  
623 rRNA genes (purple). The outer circles indicate the positions of protein coding genes on the  
624 plus strand (dark blue) and minus strand (light blue).

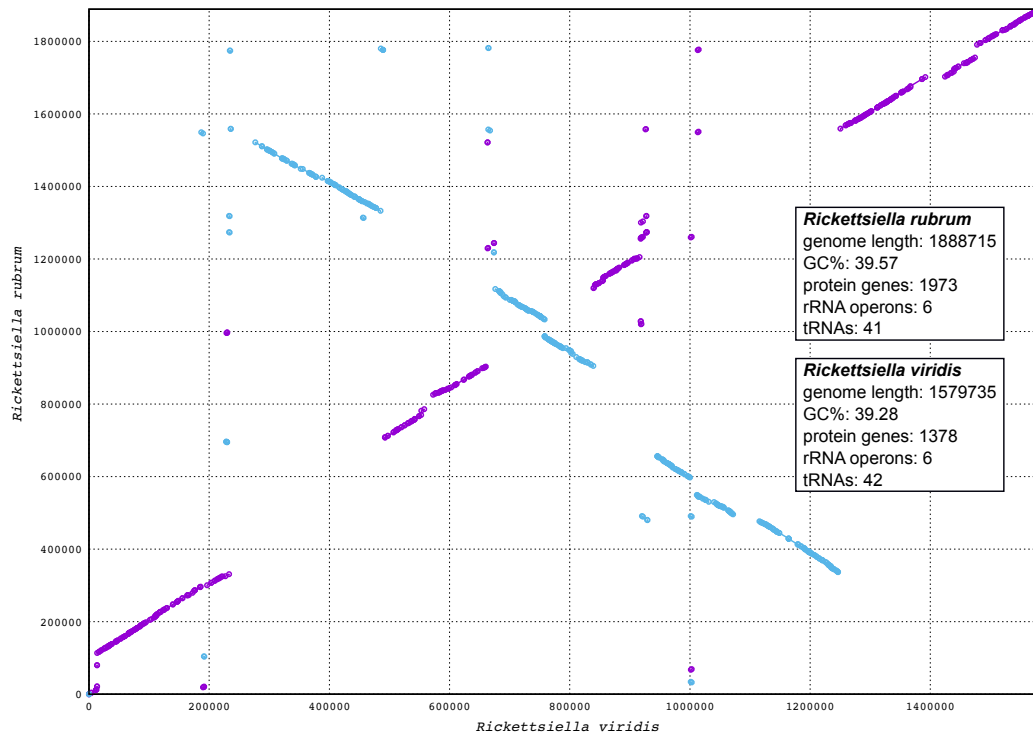
625

626

627



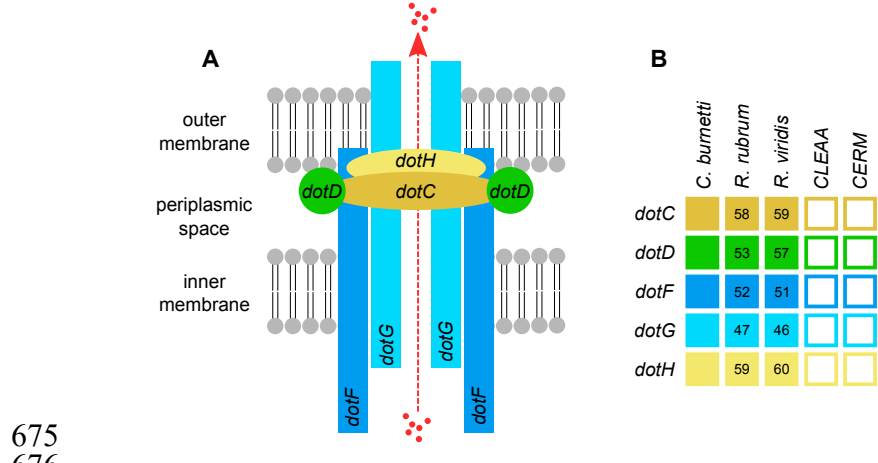
628  
629  
630 **Figure 4.** Phylogenetic placement of *R. rubrum* in the Gammaproteobacteria. The maximum  
631 likelihood phylogeny is inferred from 16S rDNA sequences. Statistical support is shown at  
632 each node from 1,000 bootstrap replicates. Scale bar represents 0.02 substitutions per site.  
633  
634  
635  
636  
637  
638  
639  
640  
641  
642  
643  
644  
645  
646  
647  
648  
649  
650  
651

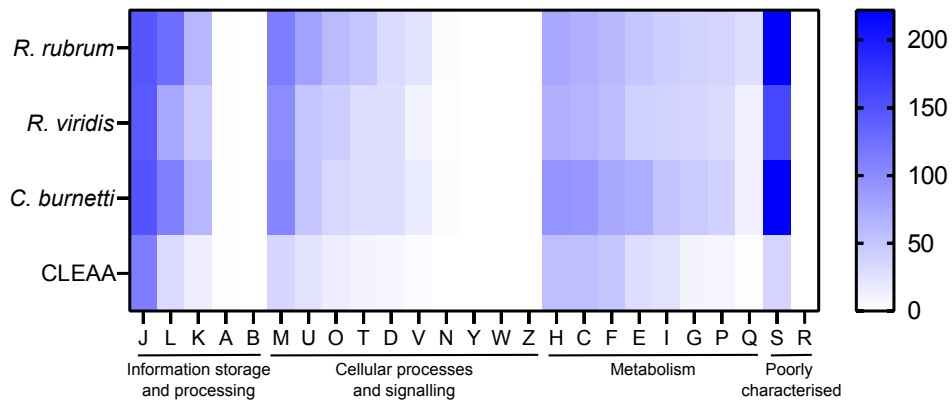


652  
653

654 **Figure 5.** Synteny analysis between *R. rubrum* and *R. viridis* genomes. The *R. rubrum*  
655 genome is represented on the y axis and the *R. viridis* genome is represented on the x axis.  
656 Blue and purple lines represent synteny between the two genomes, with blue lines being  
657 inverted in *R. rubrum* relative to *R. viridis*.

658  
659  
660  
661  
662  
663  
664  
665  
666  
667  
668  
669  
670  
671  
672  
673  
674



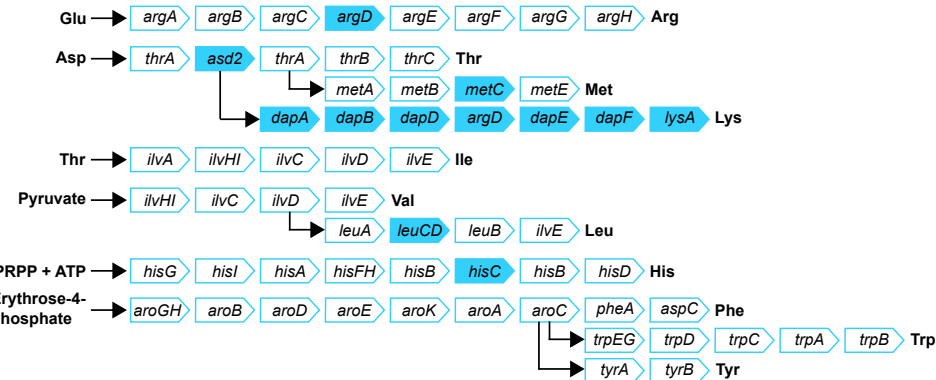


707  
708

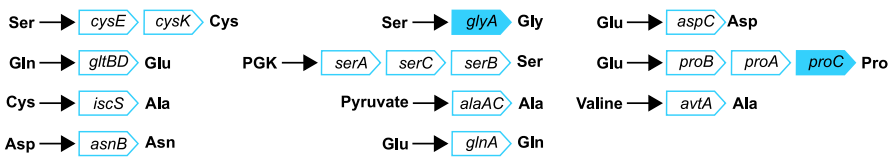
709 **Figure 7.** Heatmap comparison of Cluster of Orthologous Groups (COG) frequency in *R.*  
710 *rubrum* and related bacteria. Abbreviations for functional categories are as follows: **J**,  
711 Translation, ribosomal structure and biogenesis; **L**, Replication, recombination and repair; **K**,  
712 Transcription; **A**, RNA processing and modification; **B**, Chromatin structure and dynamics; **M**,  
713 Cell wall/membrane/envelope biogenesis; **U**, Intracellular trafficking, secretion, and vesicular  
714 transport; **T**, Signal transduction mechanisms; **O**, Posttranslational modification, protein  
715 turnover, chaperones; **D**, Cell cycle control, cell division, chromosome partitioning; **V**, Defense  
716 mechanisms; **N**, Cell motility; **Y**, Nuclear structure; **W**, Extracellular structures; **Z**,  
717 Cytoskeleton; **H**, Coenzyme transport and metabolism; **C**, Energy production and conversion;  
718 **F**, Nucleotide transport and metabolism; **E**, Amino acid transport and metabolism; **I**, Lipid  
719 transport and metabolism; **G**, Carbohydrate transport and metabolism; **P**, Inorganic ion  
720 transport and metabolism; **Q**, Secondary metabolites biosynthesis, transport and catabolism;  
721 **S**, Function unknown; **R**, General function prediction only. Scale bar (0, white; 200, blue)  
722 indicates number of COGs in each category.

723  
724  
725  
726

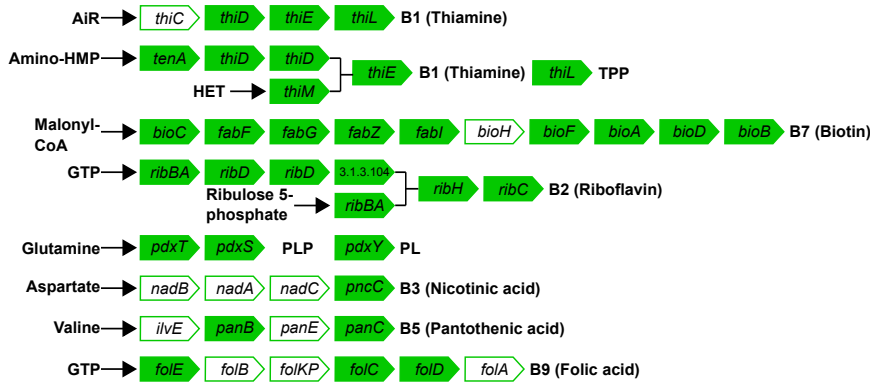
**A Essential amino acids**



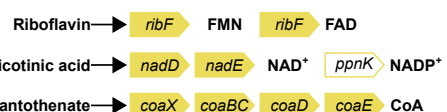
**B Non-essential amino acids**



**C Vitamins**



**D Cofactors**



727  
728

729 **Figure 8.** Biosynthetic pathways for synthesis of **A** essential amino acids; **B** non-essential  
730 amino acids; **C** vitamins and **D** cofactors in *R. rubrum*. Gene names are indicated in arrowed  
731 rectangles, coloured arrows show genes present in *R. rubrum*; missing genes are shown in  
732 white arrows.

733  
734

735  
736

737  
738

739  
740

741  
742

743  
744

745 **Tables**

746

747 **Table 1.** General genomic features of *R. rubrum* and allied Gammaproteobacteria

748

|                                   | <i>R. rubrum</i> | <i>R. viridis</i> | <i>C. burnetii</i><br>RSA 493 | <i>E. coli</i> K-12 |
|-----------------------------------|------------------|-------------------|-------------------------------|---------------------|
| <b>Genome size, Mbp</b>           | 1.89             | 1.58              | 2.00                          | 4.64                |
| <b>G+C %</b>                      | 39.6             | 39.3              | 42.7                          | 50.8                |
| <b>Protein-coding genes</b>       | 1973             | 1362              | 1798                          | 4242                |
| <b>Number of COGs<sup>#</sup></b> | 1322             | 1033              | 1293                          | 3812                |
| <b>Coding density %</b>           | 91.0             | 87.1              | 77.7                          | 85.8                |
| <b>Average gene size</b>          | 870              | 1010              | 862                           | 939                 |

749

750 #COG, Cluster of Orthologous Groups

751

752

753

754

755

756

757

758

759

760

761

762

763

764

765

766

767